SELECTED ASPECTS OF THE STRUCTURE OF EXOTIC NUCLEI AND NEW OPPORTUNITIES WITH GRETINA*

A.O. Macchiavelli

Nuclear Science Division, Lawrence Barkeley National Laboratory
Berkeley CA 94720, USA

(Received February 13, 2013)

In this contribution, we present recent results related to the quadrupole collectivity in neutron rich carbon isotopes. $B(E2)$ transitions strengths derived from lifetime measurements are interpreted in a seniority scheme, indicating an increase role of proton excitations due to the reduction of the $p_{3/2}$–$p_{1/2}$ spin–orbit splitting. We also discuss the evolution of the $N=40$ shell closure with isospin and report on preliminary results of Coulomb Excitation experiments on ^{66,68}Fe and ^{64}Cr. Finally, a short review of the gamma-ray tracking technique and a status report of GRETINA are presented. Some aspects of the exciting physics campaign being carried out at NSCL/MSU are discussed.

DOI:10.5506/APhysPolB.44.359
PACS numbers: 27.20.+n, 27.50.+e, 21.10.Tg, 23.20.Lv

1. Introduction

The structure of nuclei far from the stability line is a central theme of research in nuclear physics, both in experiment and theory. Radioactive beam facilities and novel detector systems are unique tools to produce and study these nuclei, and together with new developments in nuclear theory they provide a framework to understand the properties of these exotic nuclei.

Much of the information we have on the atomic nucleus has been obtained near the stability line and thus, by reaching the extremes of the nuclear landscape we expect to learn more about the different contributions to the nuclear force, their dependence with isospin and the effects associated with continuum coupling as one approaches the limits of weak binding.

* Presented at the Zakopane Conference on Nuclear Physics "Extremes of the Nuclear Landscape", Zakopane, Poland, August 27–September 2, 2012.

An interesting aspect that has drawn much interest in recent years and was well covered in this conference [1] is the evolution of shell structure and collectivity far from stability. In this contribution, we focus on two selected topics along those lines: quadrupole collectivity in the carbon isotopes and the new island of inversion near ^{64}Cr.

A brief review of gamma-ray tracking and the status of GRETINA will be also discussed.

2. $B(E2)$ transition strengths of neutron-rich carbon isotopes

The neutron-rich carbon isotopes, which are experimentally accessible up to the neutron dripline, provide a unique opportunity to study the evolution of nuclear structure and the coupling of neutron and proton degrees of freedom.

The even-mass neutron-rich carbon isotopes have received considerable attention since the initial claim of a quenched $B(E2)$ value and large asymmetries in the proton and neutron quadrupole matrix elements were reported and interpreted as evidence of the decoupling of the valence neutrons from the core [2].

Subsequent work [3] and more recently [4, 5] a series of Recoil Distance Method experiments carried out at the National Superconducting Cyclotron Laboratory (NSCL) at Michigan State University, reported values for the $B(E2)$s that do not support the scenario of an anomalous decoupling of the valence neutrons from the core and can be understood without resorting to new or unexpected phenomena. The current experimental data is reviewed in Fig. 1 which also includes a shell model calculations with the

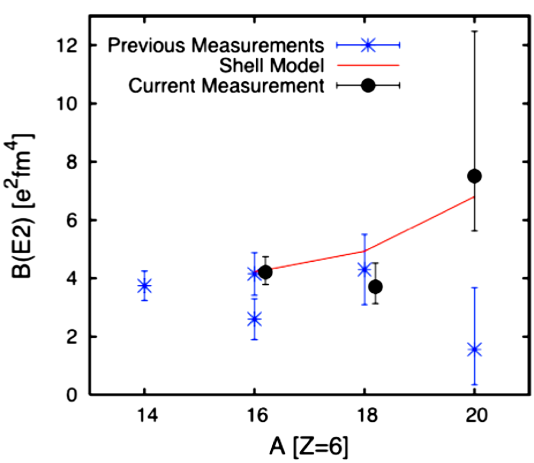

Fig. 1. Summary of $B(E2)$ values in the carbon isotopes.

WBT interaction using effective charges from [6]. Contrary to a decrease in the quadrupole collectivity, which could signal a decoupling of neutrons and protons, the $B(E2)$s show an increase towards ^{20}C.

Can we understand this behavior by considering a seniority inspired scheme? [7–9]. The rather constant energy of the 2^+ state suggests that such a description may be adequate. Moreover, since pairing ($\Delta \approx 3$ MeV) is expected to dominate over the single particle spacing, $E_{s_{1/2}} - E_{d_{5/2}} \approx 1.5$ MeV we further consider the neutron configuration $(ds)^n$ taking the ds levels as an effective j^n shell. A proton particle–hole excitation across the gap between the $p_{1/2}$ and $p_{3/2}$ levels can also contribute to the $B(E2)$ as schematically shown in Fig. 2.

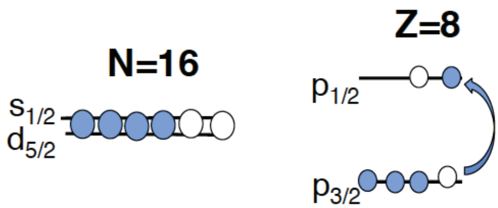

Fig. 2. A seniority scheme for the C isotopes.

The wave function of the lowest 2^+ in the carbons is thus assumed to be of the form

$$\left|2_1^+\right\rangle = \alpha \left|\nu(ds)^n\right\rangle + \beta \left|\pi p_{3/2}^{-1} p_{1/2}^{1}\right\rangle \tag{1}$$

with the $B(E2)$ for the neutrons following the behavior of the seniority scheme, *i.e.*

$$B(E2)_n = \frac{n(2j+1-n)}{2(2j-1)} B(E2)_{n=2} \,. \tag{2}$$

We fix the proton $E2$ matrix element from ^{14}C and the proton amplitude in ^{16}C to 11% as measured in the one-proton knockout reaction from ^{17}N [4].

In Fig. 3, the data are compared to the results of the seniority approach which requires an increase in the proton contributions to reproduce the trend of the experimental points. The adjusted proton amplitudes are 13% and 31% in ^{18,20}C respectively.

The increase in the proton component can be probed by g-factor measurements. With the wave function in Eq. (1) the g-factor of the 2^+ state is

$$g_{2^+} = \alpha^2 g_\nu + \beta^2 g_\pi \,. \tag{3}$$

From ^{15}C we determine $g_\nu \approx -0.69$ and from ^{13}B and ^{15}N $g_\pi \approx 1.45$. As expected, and seen in Fig. 4 the evolution of the g-factors clearly reflects the increase of the proton amplitude. Currently, these experiments are very

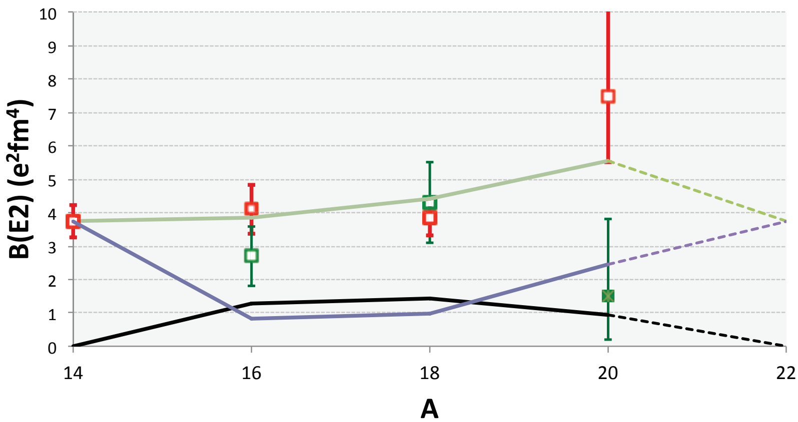

Fig. 3. $B(E2)$ values in carbon isotopes and the results of the seniority approach (light gray/green line). Contributions from neutrons (black) and protons (dark gray/purple) are shown.

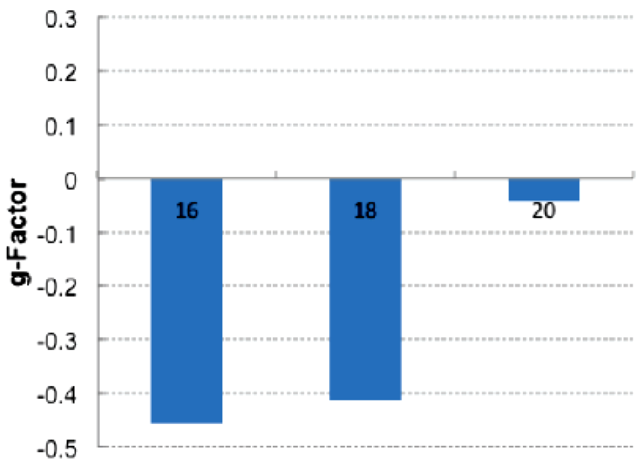

Fig. 4. Predicted g-factors for the 2^+ states in ^{16,18,20}C.

challenging given available intensities, in particular for ^{20}C. However, the proton occupancies can also be studied by measuring spectroscopic factors from 1-p knockout $^{A+1}$N to ^{A}C, since for the specific case of carbons, population of 2^+ proceeds only through the proton component. The relative cross-sections to populate the ground-state and the 2^+ can be expressed

$$\sigma\left(2^+\right)/\sigma\left(0^+\right) \approx 5/2\beta^2 \tag{4}$$

and these experiments are possible.

Do we understand the increased role of the proton component? The answer is yes and it can be attributed to a reduction in the $p_{3/2}$–$p_{1/2}$ spin–orbit splitting as neutrons are added in the *ds* shell. A similar case in the Sr–Zr region has been discussed in [10]. Using, for example, the Schiffer–True interaction, we can estimate a change in the splitting of the order of

$$\Delta E_{p3/2-p1/2} = (-0.35 \text{ MeV [Tensor]} - 0.05 \text{ MeV [Central]})n_{d5/2} \qquad (5)$$

accounting for approximately -2.5 MeV between ^{14}C and ^{20}C. Because of the similar radial forms of the $p_{3/2}$ and $p_{1/2}$ orbits, the major contribution to the monopole term arises from the tensor part of the effective interaction.

3. The island of inversion around ^{64}Cr

Another region of recent experimental and theoretical interest are the neutron-rich isotopes near $N = 40$, below the $_{28}$Ni isotopes. In analogy to the 'island of inversion' nuclei near $N = 20$, the Fe and Cr isotopes in this region have been experimentally observed to exhibit increasingly collective behavior, rather than the near-magic behavior expected assuming a robust $N = 40$ subshell gap. The development of collectivity moving from $_{28}$Ni to $_{26}$Fe and $_{24}$Cr is understood as a result of a narrowing $N = 40$ shell closure and enhancement of quadrupole collectivity through promotion of neutron pairs across the subshell gap. With the removal of protons from the $1f_{7/2}$ orbital, the attractive interaction between $1f_{7/2}$ proton holes and neutrons in the $1g_{9/2}$ and $2d_{5/2}$ orbits pulls these neutron single-particle levels down in energy. Similarly, the repulsive $(\pi 1f_{7/2})^{-1} - \nu 1f_{5/2}$ interaction drives the neutron $1f_{5/2}$ orbital up, effectively quenching the $N = 40$ gap.

The quadrupole collectivity is further enhanced as a result of the nearby presence of the $\Delta j = 2$ partner orbitals $1\nu g_{9/2}$ and $2\nu d_{5/2}$, members of a quasi-SU3 sequence, which is known to generate collectivity [12].

The picture of structural evolution described previously is borne out by complete nuclear structure calculations, using for example state-of-the-art large-scale shell model calculations [13].

Recent experimental work in this region has been carried out to confront the theoretical predictions. Early measurements of the energy of the first 2^+ excited states in the Fe and Cr isotopes [14–17] showed a decreasing trend through $N = 40$, and recent lifetime measurements in the neutron-rich ^{64,66}Fe isotopes up to $N = 40$ [18, 19] have confirmed the collectivity in the Fe isotopes. In the lighter Cr isotopic chain, data have been more limited. Proton inelastic scattering measurements [20] provided first (indirect) confirmation of increasing collectivity up to $N = 38$, and have been recently confirmed by intermediate-energy Coulomb excitation, probing the $B(E2)$ values directly [21].

We present here the first direct measurement of the collectivity of ${}^{64}_{24}$Cr, predicted to be at the center of the new region of deformation near $N = 40$, as well as confirmation of the measured quadrupole collectivity in ^{66}Fe [19] and an extension of the $B(E2)$ systematics in the ${}_{26}$Fe isotopic chain to $N = 42$. Quadrupole collectivity was measured via determination of the $B(E2 : 0^+_1 \to 2^+_1)$ using intermediate-energy Coulomb excitation.

The measurements were performed at NSCL. Secondary radioactive ion beams containing ^{66}Fe, ^{68}Fe and ^{64}Cr were produced by in-flight fragmentation of a 130-MeV/A ^{76}Ge primary beam.

The fragments of interest were selected in the A1900 separator [22], using separate magnetic rigidity settings for the three isotopes studied and a total momentum acceptance of 2%. The resulting rare isotope beams had purities of 23% for ^{66}Fe, 6% for ^{68}Fe and 2% in the case of ^{64}Cr, with average rates for the isotope of interest of approximately 300, 20 and 2 pps respectively.

Bismuth targets used to induce projectile Coulomb excitation were located at the target position of the S800 spectrograph [23]. The reaction target in front of the S800 spectrograph was surrounded by the scintillator array CAESAR, an array of 192 CsI(Na) scintillator crystals for γ-ray detection [24]. The high granularity of the array allowed for an event-by-event Doppler reconstruction, where the angle of the emitted γ-ray was determined

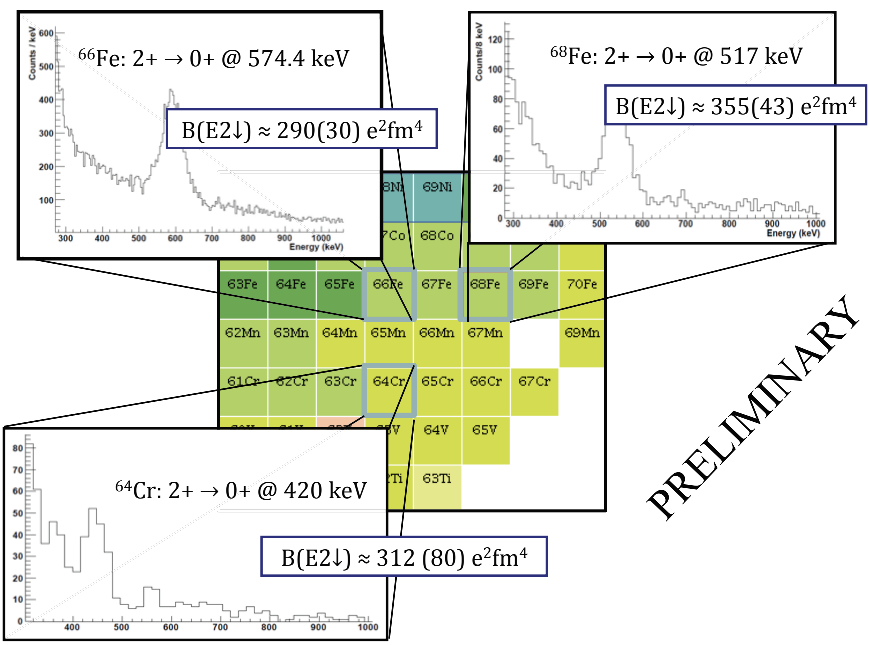

Fig. 5. Preliminary Coulex spectra and derived $B(E2)$s.

based on the position of the crystal recording the highest energy deposition in a given event. The identification of the reaction residues was performed on an event-by-event basis utilizing the detection systems of the S800 focal plane [25].

Preliminary spectra and results are shown in Fig. 5. The measured $B(E2 : 0_1^+ \to 2_1^+)$ values in ^{66,68}Fe and ^{64}Cr will provide a test of state-of-the-art theory at the predicted center of the region of collectivity below ^{68}Ni [26].

4. GRETINA

Gamma-ray spectroscopy has developed into one of the most powerful tools to study the structure of excited nuclear states and advances in gamma detection has resulted in significant new insights into the structure of nuclei.

The gamma-ray tracking technique uses highly segmented Ge detectors, and measures pulse shapes from each of the segments using fast digital electronics. These pulses are analyzed, in a procedure called signal decomposition, to determine energy, time, and three-dimensional positions of all gamma-ray interactions. This information is then used, together with the characteristics of the Compton and pair-production processes, to group and sequence the interactions points and determine the scattering path of the original gamma rays. A 4π detector array based on this novel technique would provide high efficiency ($\approx 45\%$ for a 1 MeV gamma ray), excellent peak-to-total ratio (≈ 0.6), and accurate position resolution (2 mm), increasing the detection sensitivity of the spectrometer by several hundreds compared to current arrays used in nuclear physics research [27, 28].

GRETINA [29], a first implementation of such an array using coaxial crystals (6×6 segments) and covering 1π solid angle, was completed in March 2011 at LBNL and is now running its first physics campaign at NSCL/MSU. A similar system developed in Europe, the AGATA demonstrator [30], is currently running a campaign at GSI. In spite of the limited solid angle coverage a compelling physics program has been identified for these devices.

The new technological advances which make the tracking detector possible are: the fabrication of highly segmented Ge detectors, fast digital electronics, fast signal analysis algorithms, and computing power. It seems clear that the unprecedented capabilities of a tracking detector array will extend the science reach of existing and future accelerator facilities such as FRIB in the US. In addition to nuclear physics research, tracking detectors have broad applications in medical imaging, homeland security, and environmental monitoring.

GRETINA uses coaxial Ge crystals with tapered hexagonal shapes. It consists of seven modules each containing four 36-fold segmented crystals. The 28 crystals cover a quarter of the total 4π solid angle. GRETINA is funded by the U.S. Department of Energy, and its construction began in 2007 with LBNL being the lead laboratory. A number of U.S. Universities and National Laboratories are involved in this collaborative effort: Argonne National Laboratory (trigger electronics, and data analysis/monitoring software), Michigan State University (detector testing and characterization), Oak Ridge National Laboratory (liquid nitrogen system and signal analysis software), and Washington University (target chamber).

The central part of GRETINA are the Ge detector modules, one of them shown in Fig. 6. These modules have been under extensive performance tests, including energy, time and position resolution measurements, as well as pulse rise time and cross talk properties. The position resolutions, as measured using collimated sources and data analyzed with the latest signal decomposition and tracking algorithms, are about 1–2 mm RMS depending on location of the interaction point in the crystal. The detector support structure consists of two 50-inch diameter quarter spheres and a mechanism for translation and rotation that positions detectors within 0.4 mm. The data acquisition system include 100 MHz 14-bit digitizer modules and trigger modules [31, 32]. There are more than 1000 channels of digitizers for all the segments and central contacts signals. The computer cluster to perform signal decomposition and tracking consists of 60 nodes each one with 8 cores.

Fig. 6. GRETINA quad module showing the 4 canisters inside the cryostat.

The construction of GRETINA was completed in March 2011. Since then, a number of engineering runs have been carried out at the 88-Inch Cyclotron of LBNL to test the system under various realistic experimental conditions, to improve its performance, and to further characterize its properties. A series of commissioning runs at the target position of the Berkeley Gas-filled Separator (BGS) followed with the aim of of probing the structure of heavy nuclei near ^{254}No. The reaction ^{144}Sm + ^{36}Ar was used to produce ^{176}Pt as a test case for the GRETINA-BGS coincidence set up where the compound residues were detected at the focal plane of BGS. A spectrum from this run is shown in Fig. 7. Analysis of the ^{254}No data is still in progress.

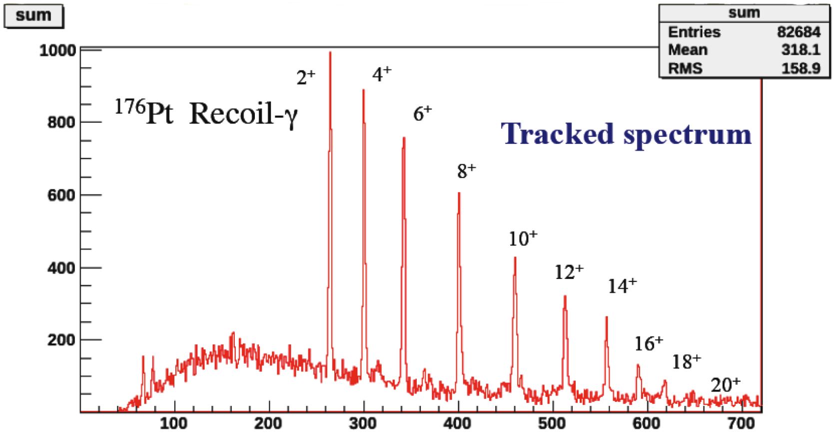

Fig. 7. Spectrum of ^{176}Pt in coincidence with recoils at the focal plane of the BGS.

In April 2012, GRETINA moved to Michigan State University for a fast beams campaign at the S800 spectrograph. 24 experiments were approved for a total of 3350 hours of beam time addressing many subjects of current interest: Shell-evolution and Collectivity, Mirror-symmetry, Giant Resonances and Nuclear Astrophysics. These experiments with fast beams take advantage of the improved Doppler reconstruction and resolving power of the array. An example of the spectrum quality is illustrated in Fig. 8 from the commissioning run [33]. Gamma rays from ^{28}Si moving at $v/c \approx 40\%$ are shown after Doppler reconstruction and tracking.

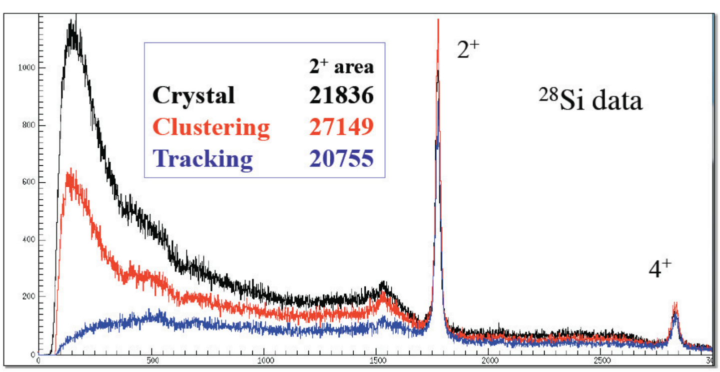

Fig. 8. Reconstructed spectrum for ^{28}Si from the commissioning run at NSCL. The improved quality after tracking is observed.

In 2013, GRETINA will relocate to ANL for studies of exotic nuclei using stable beams and neutron-rich beams from CARIBU.

We look forward to exciting physics results from these science campaigns that take advantage of the unique capabilities available at these facilities.

The next step is the construction of a 4π array. The U.S. and European nuclear physics communities are actively working to start building GRETA and AGATA. These arrays will provide unique opportunities to advance studies in nuclear structure, nuclear reactions, and fundamental symmetries. In the U.S., GRETA obtained a strong endorsement in the 2007 U.S. DOE/NSF NSAC Long Range Planning activities and it is our hope that with proper funding, it will be ready for day one operations at FRIB.

It was a great pleasure for me to attend this conference in Zakopane and visit Poland for the first time. I would like to thank the Organizing Committee and Robert Janssens (Convener of the session on *Evolution of Nuclear Structure in Neutron-rich Nuclei*) for their kind invitation. I would like to acknowledge many discussions with my colleagues at Berkeley on the subjects covered in this article. Last, but not least, I would like to thank Heather Crawford, Marina Petri, I-Yang Lee, and Dirk Weisshaar for their help in preparing the presentation. This work is supported under contract number DE-AC02-05CH11231.

REFERENCES

[1] F. Nowacki, T. Otsuka, Th. Papenbrok, O. Sorlin, talks at this conference, not submitted to the proceedings.

[2] N. Imai *et al.*, *Phys. Rev. Lett.* **92**, 062501 (2004).

[3] M. Wiedeking *et al.*, *Phys. Rev. Lett.* **100**, 152501 (2008).

[4] M. Petri *et al.*, *Phys. Rev. Lett.* **107**, 102501 (2011); *Phys. Rev.* **C86**, 044329 (2012).

[5] P. Voss *et al.*, *Phys. Rev.* **C86**, 011303(R) (2012).

[6] H. Sagawa *et al.*, *Phys. Rev.* **C70**, 054316 (2004).

[7] I. Talmi, *Simple Models of Complex Nuclei*, Harwood Academic Publishers, 1993.

[8] I. Morales *et al.*, *Phys. Lett.* **B703**, 606 (2011).

[9] M. Caprio *et al.*, *Phys. Rev.* **C85**, 034324 (2012).

[10] P. Federman *et al.*, *Phys. Lett.* **B140**, 269 (1984).

[11] T. Otsuka *et al.*, *Phys. Rev. Lett.* **95**, 232502 (2005).

[12] A.P. Zuker, *et al.*, *Phys. Rev.* **C52**, R1741 (1995).

[13] S.M. Lenzi *et al.*, *Phys. Rev.* **C82**, 054301 (2010).

[14] O. Sorlin *et al.*, *Eur. Phys. J.* **A16**, 55 (2003).

[15] A. Gade *et al.*, *Phys. Rev.* **C81**, 051304(R) (2010).

[16] M. Hannawal *et al.*, *Phys. Rev. Lett.* **82**, 1391 (1999).

[17] P. Adrich *et al.*, *Phys. Rev.* **C77**, 054306 (2008).

[18] J. Ljungvall *et al.*, *Phys. Rev.* **C81**, 061301(R) (2010).

[19] W. Rother *et al.*, *Phys. Rev. Lett.* **106**, 022502 (2011).

[20] N. Aoi *et al.*, *Phys. Rev. Lett.* **102**, 012502 (2009).

[21] T. Baugher *et al.*, *Phys. Rev.* **C86**, 011305(R) (2012).

[22] D.J. Morrissey *et al.*, *Nucl. Instrum. Methods Phys. Res.* **B204**, 90 (2003).

[23] D. Bazin *et al.*, *Nucl. Instrum. Methods Phys. Res.* **B204**, 629 (2003).

[24] D. Weisshaar *et al.*, *Nucl. Instrum. Methods Phys. Res.* **A624**, 615 (2010).

[25] J. Yurkon *et al.*, *Nucl. Instrum. Methods Phys. Res.* **A422**, 291 (1999).

[26] H.L. Crawford *et al.*, in preparation.

[27] I.Y. Lee, *Nucl. Instrum. Methods Phys. Res.* **A422**, 195 (1999).

[28] M.A. Deleplanque *et al.*, *Nucl. Instrum. Methods Phys. Res.* **A430**, 292 (1999).

[29] S. Paschalis *et al.*, *Instrum. Methods Phys. Res.*, in press.

[30] S. Akkoyun, *et al.*, *Nucl. Instrum. Methods Phys. Res.* **A668**, 26 (2012).

[31] M. Cromaz *et al.*, *Nucl. Instrum. Methods Phys. Res.* **A597**, 233 (2008).

[32] J. Anderson *et al.*, *IEEE Trans. Nucl. Sci.* **56**, 258 (2009).

[33] D. Weisshaar *et al.*, NSCL Experiment 11007.